IEEE Access
Multidisciplinary | Rapid Review | Open Access Journal

Received July 22, 2018, accepted August 24, 2018, date of publication August 31, 2018, date of current version September 21, 2018.

Digital Object Identifier 10.1109/ACCESS.2018.2868058

Improved Method to Obtain the Online Impulse Frequency Response Signature of a Power Transformer by Multi Scale Complex CWT

ZHONGYONG ZHAO[1], CHAO TANG[1], CHENGUO YAO[2], (Member, IEEE), QU ZHOU[1], LINGNA XU[1], YINGANG GUI[1], AND SYED ISLAM[3], (Senior Member, IEEE)

[1]College of Engineering and Technology, Southwest University, Chongqing 400716, China
[2]State Key Laboratory of Power Transmission Equipment and System Security and New Technology, Chongqing University, Chongqing 400044, China
[3]School of Electrical Engineering and Computing, Curtin University, Perth, WA 6102, Australia

Corresponding author: Zhongyong Zhao (zhaozy1988@swu.edu.cn)

This work was supported in part by the National Natural Science Foundation of China under Grant 51807166 and in part by the Fundamental Research Funds for the Central Universities under Grant SWU118031.

ABSTRACT Online impulse frequency response analysis (IFRA) has proven to be a promising method to detect and diagnose the transformer winding mechanical faults when the transformer is in service. However, the existing fast Fourier transform (FFT) is actually not suitable for processing the transient signals in online IFRA. The field test result also shows that the IFRA signature obtained by FFT is easily distorted by noise. An improved method to obtain the online IFRA signature based on multi-scale complex continuous wavelet transform is proposed. The electrical model simulation and online experiment indicate the superiority of the wavelet transform compared with FFT. This paper provides guidance on the actual application of the online IFRA method.

INDEX TERMS Impulse frequency response, power transformers, windings, complex CWT, fast Fourier transform, electrical model.

I. INTRODUCTION

Most of the power transformers worldwide were installed in the 1980s, thus; they are reaching the ends of life cycles [1]. The failure rate of these transformers is persistently rising according to the annual report of the Power Company or the statistical analysis of some commercial and non-profit electric institutions. Transformer failure, especially catastrophic failure, will cause outages of power networks and huge economic losses [2]. Among all the reasons to induce power transformer failure, winding deformation contributes approximately one-third to the failure rate, based on the statistical data of the CIGRE working group [3]. Winding deformations, including tilting, forced bulking, free buckling, hoop tension, telescoping, etc., are largely caused by short circuit electromagnetic forces, of which the force is the outcome of the external short circuit current and the internal electromagnetic field [4]. Besides, earthquake, careless transportation, aging of insulation material, and explosion of combustible gas in transformer oil could also be reasons for giving rise to winding deformation faults [5]. Winding deformation will have a limited impact on the normal operation of power transformer when it is at the early stage of failure; however, minor failure will develop into the serious failure if no steps are taken. Consequently, for both operators and stakeholders, it is necessary and meaningful to timely detect and diagnose the winding deformation faults when a transformer is in service [6].

Recently, some researchers have proposed various methods for online monitoring of transformer winding deformation. The online short circuit impedance (SCI) method [7], vibration method [8], ultra-wideband (UWB) antenna method [9], Lissajous locus method [10] and online frequency response analysis (FRA) method [11], [12] have been applied in this field. Among all the methods, the FRA method has already proven to be a reliable, fast, economic and non-destructive diagnostic tool [13]; hopefully, the online FRA method may also have these potential features in the future, as indicated by the existing abundant research findings. According to the nature of the input signal, online FRA can be divided into two categories, online sweep FRA (SFRA) and online impulse FRA (IFRA) [14]. Online SFRA uses a sinuous signal as the excitation of the transformer winding, whereas the impulse signal is used as the excitation signal in online IFRA. Normally, online IFRA uses

controllable or uncontrollable high voltage impulse signals. The controllable impulse signal is injected and coupled into the winding, while the uncontrollable signal, such as lightning or switching overvoltage, is propagated to the transformer bushing via the HV line [12].

Compared with the current SFRA technique, IFRA has the advantages of smaller energy injection and less time consumption that give it potential for online application. For different uncontrollable excitations, Leibfried and Feser [15] used the switching transient signal to excite power transformer, while Wang *et al.* [16] introduced the lightning over-voltage as the excitation. For the controllable excitation method, De Rybel [17] proposed an apparatus for online monitoring power transformer by injecting the high frequency signal from the busing tap. Afterwards, Yao *et al.* [18] established a capacitive coupling sensor (CCS) and another apparatus for injecting the nanosecond pulse to the transformer windings. Moreover, Bagheri *et al.* [19] analyzed the impact of the capacitive bushing on the online FRA signature by theoretical analysis and experimental validation.

However, most of the works mentioned above are focused on the implementation of the diagnostic method itself. Few researchers have switched their attention to the FRA signature, where a mathematical approach is normally applied to construct the IFRA signature from the measured time domain transient signals. Generally, to obtain an accurate IFRA signature, the simplest approach is improving the amplitude of the excitation pulse to be as high as possible to improve the SNR of the response signal. However, this poses a significant challenge to the solid-state pulse generator manufacturer because the design difficulty and cost are drastically increased with the increase in pulse amplitude, and causes great worries to the Power Company for using excitation pulses with extremely high amplitude. Thus, the existing amplitude of excitation voltage varies from several hundreds of volts to a few thousand volts at the moment [18]. Therefore, a problem that the measured response signal with certain SNR is sometimes noisy has emerged.

At present, fast Fourier transform (FFT) is the primary tool for processing the measured time domain signals and obtaining the online IFRA signatures. However, problems still exist.

- It is well known that FFT is suitable for processing the steady-state signal because of the sinusoidal basis of FFT. The measured signal in IFRA is the transient signal. Using FFT to process the IFRA signals is actually not proper.
- Some practice shows the IFRA signature calculated by FFT obtained from noisy transient signals might be fuzzy, and the key information of the resonance of IFRA signature will be missing [18], [20]. With an indistinct IFRA signature and the false resonant points, it is impossible for power utility personnel to make an appropriate diagnosis decision for power transformer winding defamation, even for experienced staff.

To solve the above problems, Gómez-Luna *et al.* [21], [22] firstly introduced continuous wavelet transform (CWT) to obtain the IFRA signature from the transient signals. The wavelet transform is a multi-resolution analysis approach with excellent time-frequency localization characteristic. Compared with FFT, the basis of a wavelet is naturally convergent, making it more suitable for processing non-steady state signals. However, the used mother wavelet is a real wavelet, and the error will be generated because of the shift variance of wavelet coefficients when the wavelet is applied for decomposing the signals.

In view of the above background, this paper proposes and studies an improved method based on multi scale complex CWT (CCWT) to obtain the online IFRA signature of power transformers. Use of the complex wavelet transform can solve the above problems. The remainder of this paper is organized as follows. First, the basic principle of online IFRA and multi scale CCWT is introduced in Section II. Next, Section III proposes the simulation validation of an equivalent electrical model of winding, followed by several experimental validations of the proposed method in Section IV. The conclusions of this study are summarized in Section V.

II. BASIC PRINCIPLE

A. BRIEF INTRODUCTION OF ONLINE IFRA

A simple diagram of the online IFRA method using Y-Y connection windings as an example is depicted in Fig. 1. The HV and LV buses are represented by the equivalent characteristic impedance considering its distributed parameter features under a high frequency signal. A capacitive coupling sensor (CCS), which functions as an electrode plate of coaxial cylindrical capacitor, is wrapped around the bushing external insulation layer. The controllable high voltage nanosecond pulses are injected to the terminal of transformer winding via the capacitance formed by the CCS and the transformer bushing. The use of CCS erases the low frequency data of online IFRA signature; this effect was described in [19]

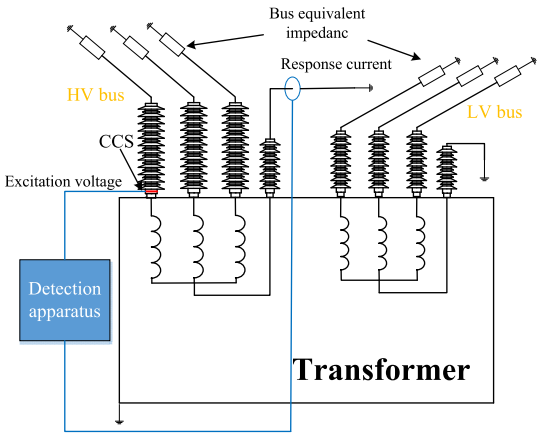

FIGURE 1. Wiring of the online IFRA method applied in a running transformer.

and [23]. The IFRA implementation on winding Wye connection (with neutral point) and Delta connetion (without neutral point) was recommended in [18]. The impact of CCS on the bushing external insulation was described in [24]. More detailed information about the diagnostic system and the practical application can be found in [18].

At present, the method to obtain the online IFRA signature from the transient signal is given by Equation (1) ∼ (3) [25], [26],

$$V_{\text{in}}(k) = \sum_{n=0}^{N-1} V_{\text{in}}(n)\, \mathrm{e}^{-\mathrm{j}\frac{2\pi}{N}kn} \tag{1}$$

$$R_{\text{out}}(k) = \sum_{n=0}^{N-1} R_{\text{out}}(n)\, \mathrm{e}^{-\mathrm{j}\frac{2\pi}{N}kn} \tag{2}$$

$$H(f) = 20\lg \frac{|R_{\text{out}}(k)|}{|V_{\text{in}}(k)|} \tag{3}$$

where $V_{\text{in}}(n)$ is the N points sampling signal of the time domain excitation voltage, and $V_{\text{in}}(k)$ is the FFT of $V_{\text{in}}(n)$; $R_{\text{out}}(n)$ is the N points sampling signal of the time domain response signal, and can be voltage or current, depending on the variable connection types of transformer winding [13], [18]; $R_{\text{out}}(k)$ is the FFT of $R_{\text{out}}(n)$; $H(f)$ is the online IFRA signature (amplitude versus frequency).

B. BASIC PRINCIPLE OF MULTI SCALE CCWT

A series of wavelet sequences can be obtained by translating and dilating the mother wavelet $\psi(t)$, and the signal can be decomposed into different frequency components, as described by Equation (4) [21], [27],

$$\psi_{\text{a,b}} = \frac{1}{\sqrt{a}}\psi\left(\frac{t-b}{a}\right) \tag{4}$$

where b is the translation factor, and a is the scale factor. a and b determine the position of the time-frequency window in the frequency domain and the time domain, respectively.

For any quadratic integration function $f(t) \in L^2(R)$, the CWT of $f(t)$ is defined as follows:

$$WT_f(a,b) = \frac{1}{\sqrt{a}}\int_{-\infty}^{+\infty} f(t)\,\psi^*\left(\frac{t-b}{a}\right)\mathrm{d}t \tag{5}$$

The wavelet transform is conducted in the scale domain, and scale should be translated to the pseudo frequency, as shown in Equation (6),

$$f_a = \frac{f_c f_s}{a} \tag{6}$$

where f_c is the center frequency of the mother wavelet; f_s denotes the sampling rate of the signal; f_a is the pseudo frequency, which corresponds to the scale a and normally functions as the actual frequency.

Suppose the time domain excitation and the response signal of IFRA test are represented by $V_{\text{in}}(t)$ and $R_{\text{out}}(t)$, respectively; the CWT coefficients of $V_{\text{in}}(t)$ and $R_{\text{out}}(t)$ are $WT_{\text{in}}(\omega, b)$ and $WT_{\text{out}}(\omega, b)$, respectively. According to the definition of the marginal spectrum, the frequency spectrum distribution of the excitation and response signal can be calculated by integrating the magnitude of the wavelet coefficient in the time domain. The IFRA signature H_{IFRA} can then be obtained according to the definition of frequency response, as shown in Equation (7),

$$H_{\text{IFRA}}(\omega) = \frac{\int_{-\infty}^{+\infty} |WT_{\text{out}}(\omega, b)|\,\mathrm{d}t}{\int_{-\infty}^{+\infty} |WT_{\text{in}}(\omega, b)|\,\mathrm{d}t} \tag{7}$$

Noted that the marginal spectrum calculated from the wavelet coefficient can reflect the magnitude spectrum distribution of the signal in the frequency domain, but this distribution is not equal to the magnitude spectrum of the Fourier transform. Both spectral distributions have the same trend with the frequency variation, but differ in the amplitude. However, the wavelet transform is used to process the excitation and the response signal, both of which are simultaneously measured. The division operation can eliminate the effect of the magnitude difference, and the obtained IFRA signature must be the real signature of the power transformer.

C. SELECTION CRITERIA OF MOTHER WAVELET

The Morlet wavelet usually serves as the mother wavelet of time-frequency analysis. The Morlet wavelet is not orthogonal and biorthogonal, strictly speaking, and it does not have compact support; nevertheless, its time-frequency local performance is excellent. The Morlet wavelet provides moderate and controllable center frequency and bandwidth, and is normally used to characterize the time-frequency characteristic of a signal [28]. In this paper, the complex Morlet wavelet is used to avoid the error generated by the shift variance of wavelet coefficients, which always exists in the real mother wavelet signal processing. The energy of the real part and the imaginary part of wavelet coefficient are complementary, and the distortion of the signal description caused by the real mother wavelet is effectively diminished. The time domain expression of the complex Morlet wavelet is given by Equation (8), and this mother wavelet has no corresponding scale function.

$$\psi(t) = \frac{1}{\sqrt{\pi f_b}} e^{2i\pi f_c t} e^{-t^2/f_b} \tag{8}$$

where f_c and f_b are the center frequency and bandwidth of the complex Morlet wavelet, respectively.

For the selection of wavelet parameters, the ''trial and error method'' is frequently used; i.e., constantly adjust the parameter value to meet the requirement of signal analysis. The selection of f_c usually allows the wavelet to approach the frequency of interest. However, the IFRA signature with wide bandwidth (1 ∼ 1000 kHz) must be obtained, multiple scales are adopted in CWT, and the center frequency of the wavelet under each scale is shifted along the frequency axis with scale variation. Thus, compared with f_b, the impact of f_c on the signal processing result is smaller. However, f_c should be slightly higher in the actual test, causing the analyzed bandwidth (1 ∼ 1000 kHz) to be located in the low frequency

TABLE 1. Equivalent electrical parameters of simulated transformer winding.

Parameters	R_s	L_s	C_s	C_g	C_{HL}	$1/G$
HV winding	1.2Ω	18μH	2.2nF	37pF	5nF	7MΩ
LV winding	0.8Ω	6μH	1.11nF	65pF	5nF	7MΩ

bands; the low frequency bands of the wavelet corresponds to a more sophisticated decomposition result.

In Equation (8), e^{-t^2/f_b} can be regarded as a Gaussian window, and f_b determines the characteristic of the standard deviation of the Gaussian function. The smaller value of f_b, the narrower is the Gaussian window, and the shorter is the effective support length of the wavelet. Correspondingly, the bandwidth of the power spectrum of the wavelet is larger, and the frequency resolution of the wavelet filter is lower. Fig. 2 illustrates the waveforms of the real part and the imaginary part of the complex Morlet wavelet under the same center frequency and variable bandwidth. The corresponding bilateral power spectrum is also presented. The above analysis result indicates that a larger f_b should be used to obtain a more accurate IFRA signature of the transformer winding.

III. SIMULATION ANALYSIS

This section demonstrates that the IFRA signature can be obtained by the proposed multi scale CCWT by simulating and analyzing an equivalent electrical model of a single-phase, shell-type transformer winding. This electrical model is shown in Fig. 3. The parameters of the electrical model are calculated by the finite element method, as listed in Tab. 1. The detailed calculation process can be found in [29] and [30]. The PSPICE software is used to simulate the model. In the model, the HV and LV windings consist of 10 disks. Each disk comprises a series resistance R_s and inductance L_s, a shunted capacitance C_s and conductance G_s. The capacitance C_{HL} between the HV winding and the LV winding with a shunted conductance G simulates the insulation condition between two windings, and mutual inductances M_{ij} between the two coils are included. The dielectric insulation (oil) between the LV winding and the core, and that between the HV winding and the tank, are simulated by a capacitance C_g and shunted dielectric conductance G.

The flow chart of the electrical model simulation and the data processing is shown in Fig. 4.

First, the excitation voltage of the HV winding is set as a sweep sinuous voltage to perform the sweep frequency analysis. As requested in the common FRA test, the frequency varies from 1 kHz to 1000 kHz, and the frequency interval is 1 kHz. The grounded current of the HV winding terminal is measured in the frequency domain to construct the SFRA signature. Obviously, this SFRA signature is the most accurate signature to describe the characteristic of the transformer winding and can be regarded as the basis for comparison.

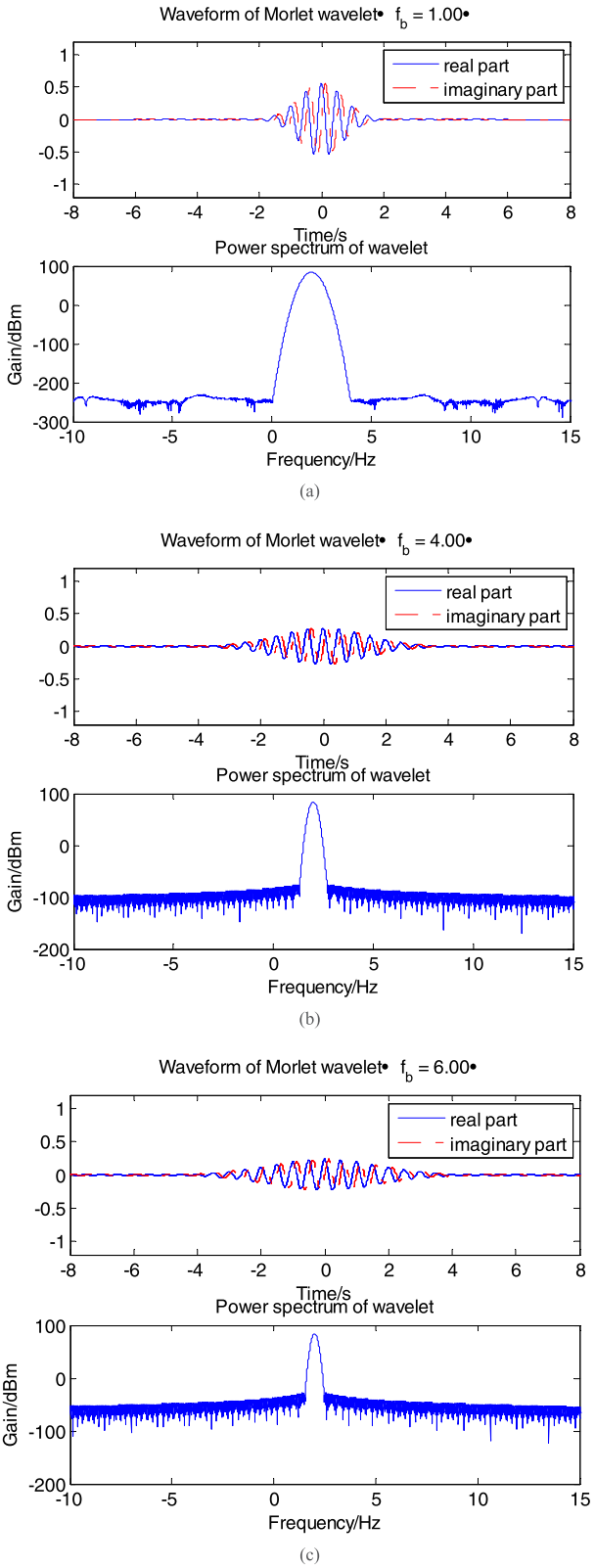

FIGURE 2. Impact of bandwidth parameter on the waveform and power spectrum of complex Morlet wavelet. (a) $f_b = 1$, (b) $f_b = 4$, (c) $f_b = 6$.

Second, a square wave pulse voltage is used as the excitation to perform the transient simulation. According to the selection criteria of the pulse key parameters in [18],

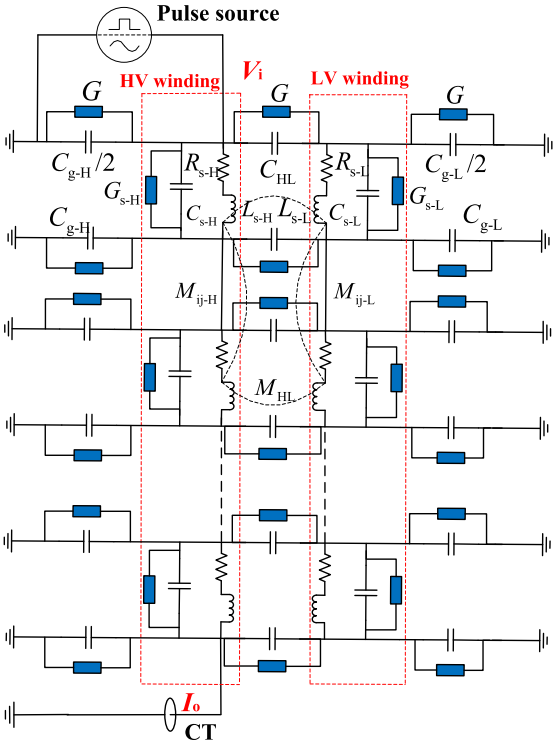

FIGURE 3. Equivalent electrical model of simulated power transformer winding [30].

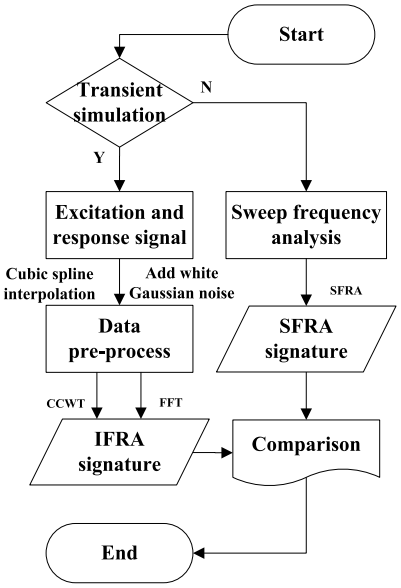

FIGURE 4. Flow chart of electrical model simulation and data processing.

the amplitude of the pulse is 500 V, the pulse width is 300 ns, and the rise and fall times are both 30 ns. The rise and fall times are emulating the actual pulse edge caused by the inductive components of the pulse forming circuit and the on/off time of semiconductor switches (MOSFET) in the Marx pulse generator. The grounded current of the HV winding terminal is measured as the response signal. Both the time domain transient excitation and response signal are used to construct an IFRA signature. It is noted that the transient analysis of PSPICE software uses the variable step-size technique to reduce the accumulative error; thus, the sampling points of the transient signals imported from PSPICE are not uniformly spaced. Cubic spline interpolation is then used to pre-process the transient signals in MATLAB software to obtain the uniformly spaced sampling data before transforming the time domain signal to the frequency domain. Afterwards, the proposed multi scale complex CWT is used to process the above signals to obtain the IFRA signature of the transformer winding. Fig. 5 shows the data processing result; it can be seen that the IFRA signature obtained by CCWT method is almost overlapped with the SFRA signature in wide frequency range. Additionally, the information of resonant points of two signatures is presented in Tab. 2. The corresponding resonant points are very similar. Both the trend of the figure and the resonant frequencies indicate that the IFRA signature of a transformer can be effectively obtained from the transient signals by the proposed CCWT method.

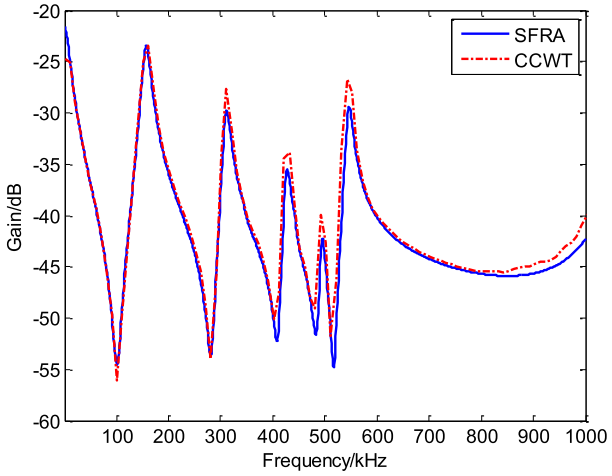

FIGURE 5. Data processing result of equivalent electrical model simulation.

TABLE 2. Frequency information of the resonance and anti-resonance for simulated ifra signature.

Resonance(kHz)			Anti-resonance(kHz)		
Frequency	SFRA	CCWT	Frequency	SFRA	CCWT
f_1	157	160	f_1'	103	101.5
f_2	312	312.4	f_2'	281	281
f_3	428	426.8	f_3'	406	402.7
f_4	496	493.1	f_4'	482	483.1
f_5	546	543.3	f_5'	518	513.2

Third, the white Gaussian noise is added to the above uniformly spaced sampling data to emulate the actual noisy transient signals. Fig. 6 shows the response signal with different values of the SNR, the numerical value after the SNR denotes the different noise levels. Obviously, the signal of SNR-10 is much noisier than the signal of SNR-20. The noisy signals are processed by the proposed CCWT, and the IFRA signature is calculated. For comparison, the IFRA signature

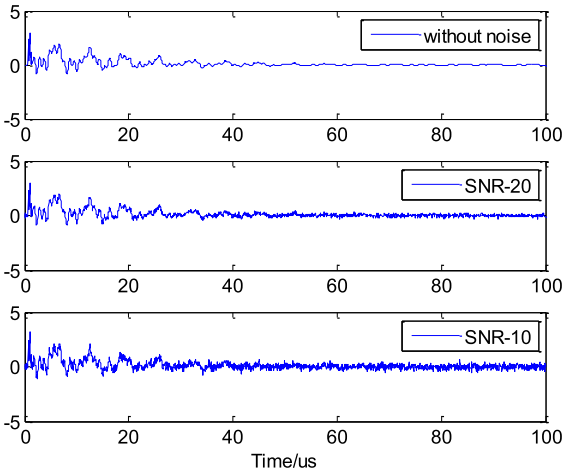

FIGURE 6. Time domain response signal with different SNR.

based on the FFT algorithm is also obtained from these noisy signals. The data processing results of the transient signals by FFT and CCWT are shown in Fig. 7; note that the analyzed frequency is extended to 3000 kHz to have a broader investigation in the high frequency band. Fig. 7 shows that the FFT-based IFRA signature is completely noisy, especially in the crucial frequency range of 500 ∼ 1000 kHz, there exist largely redundant resonant points for SNR-10, not to mention the frequencies beyond 1000 kHz. Correspondingly, the CCWT-based IFRA signature is relatively clear and smooth; the main resonant frequencies remained unchanged, which indicates the superiority of the CCWT algorithm to process the transient signal to a certain extent.

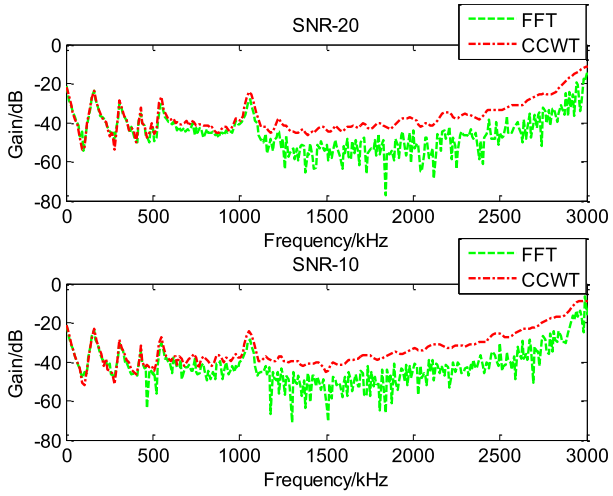

FIGURE 7. Data processing result of transient signals with different values of SNR by two methods.

IV. EXPERIMENTAL VALIDATION

A. "ONLINE EXPERIMENT" WITH TRANSFORMER NON-ENERGIZED

The power transformer experiment was conducted to verify the proposed CCWT algorithm. In this "online experiment", the excitation signal is injected into a non-energized transformer through the CCS; the term "online" is relative over the conventional offline test, in which the excitation is directly injected through the terminal of the bushing. The tested transformer is a three-phase, shell-type, specifically manufactured transformer; the rated capacity is 400 kVA; the operation frequency is 50 Hz; the rated voltage is 10/0.4 kV; and the connection sets of winding is YNyn0. A FPGA-controlled solid-state high voltage nanosecond pulse generator with adjustable output voltage of 0 ∼ 1000 V, pulse width of 1 ∼ 1000 ns based on Marx circuit is used to produce the nanosecond excitation pulse in the IFRA test. The image of the transformer, the main body of the nanosecond pulse generator, the waveforms of the adjustable excitation pulse and the wiring diagram of online experiment are shown in Fig. 8. All experiments were performed on phase *a* of LV winding.

First, the online SFRA signature of the winding phase *a* was measured. A Tektronix AFG3102 arbitrary waveform generator was used to generate the sweep sinuous signal. Considering that the amplitude of the sweep signal would be drastically reduced if the signal was directly coupled into the inner conductor of bushing by CCS, a high-voltage power amplifier TEGAM 2340 (bandwidth DC ∼ 2 MHz) was used to improve the amplitude of the sweep sinuous signal. The sweep frequency varied from 1 kHz to 1000 kHz, and the frequency interval was 2 kHz. At each frequency point, a Tektronix P5100A broadband high voltage probe and a Pearson 7790 broadband current transducer were used to measure the input sweep voltage and the output sweep current, respectively. The amplitudes of these two sinuous signals were obtained, and the gain of the online SFRA signature at a single frequency point was calculated. Subsequently, all gain values, which correspond to 500 groups of frequency points, were calculated, and the online SFRA signature was obtained.

The arbitrary waveform generator and high-voltage power amplifier were then replaced by the nanosecond pulse generator, and other apparatus and the wiring remained unchanged to perform the IFRA test. In the test, the amplitude of the output pulse from the generator was set as 900 V to improve the SNR of the response signal as far as possible, and it does not make the amplitude of the pulse excessively large, which is not accepted by utilities. The pulse width was set as 200 ns to theoretically increase the upper frequency limit of the IFRA signature to approximately 5 MHz. The transient excitation voltage and the response current were simultaneously measured, and the sampling rate was set as 50 MS/s. Moreover, the measurement was repeated 50 times under the same experimental setup, the abnormal signals were eliminated, and the average value was used as the analyzed data to reduce the influence of the external factors on the recorded data. Both CCWT and FFT algorithms were used to process the transient excitation and response signals to calculate the online IFRA data, as shown in Fig. 9. It is noted that in Fig. 9, the naming rule of signature is as follows: suppose the pattern of naming is "*ab-c*(*d*)", in which *a* can be offline/online, (offline indicates the excitation is injected

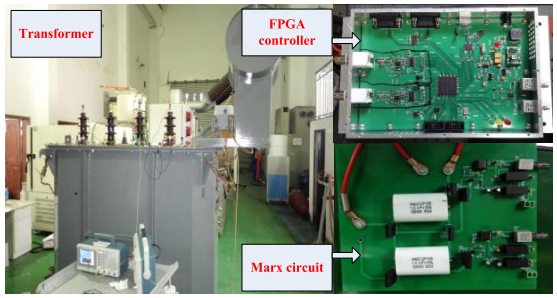

(a)

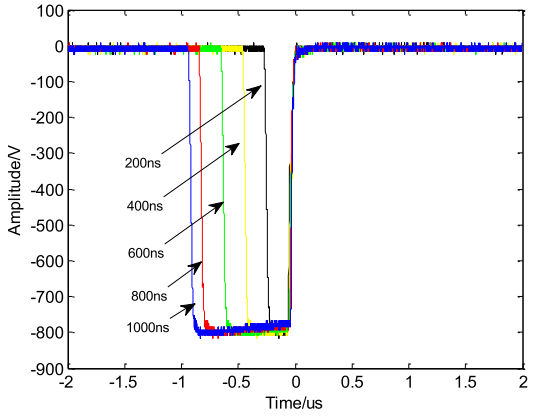

(b)

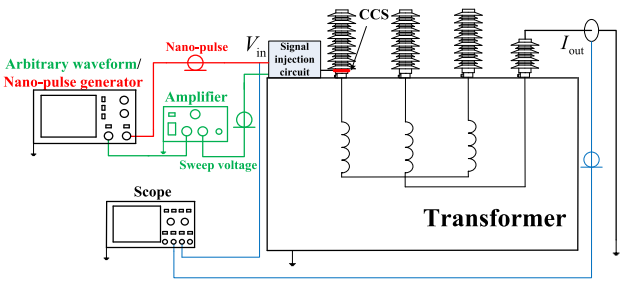

(c)

FIGURE 8. Transformer, pulse generator waveforms and wiring diagram of online experiment with transformer non-energized. (a) Actual image of tested transformer and main body of nanosecond generator. (b) Waveforms of adjustable excitation pulse. (c) Wiring diagram of online experiment with transformer non-energized.

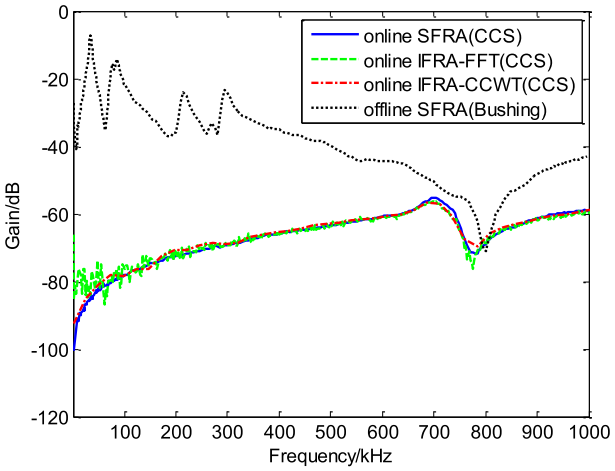

(a)

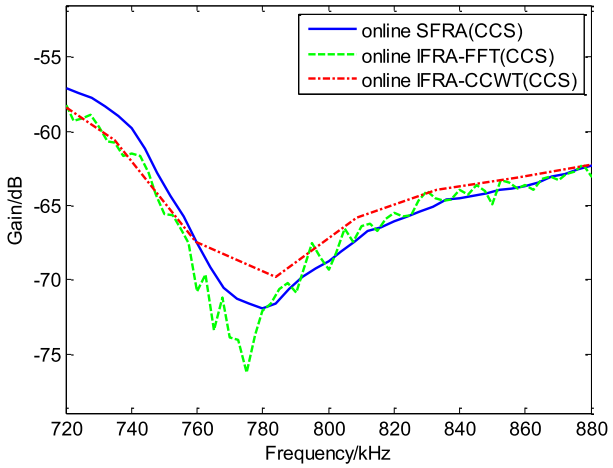

(b)

FIGURE 9. Data processing result of online experiment with transformer non-energized. (a) 1 ∼ 1000 kHz, (b) 720 ∼ 880 kHz.

through the bushing terminal, whereas online indicates the excitation is injected through CCS), and *d* denotes bushing/CCS. In addition, *b* denotes SFRA or IFRA signature, and if *b* is IFRA, then *c* denotes the signal processing algorithm (FFT/CCWT).

In Fig. 9, the online SFRA signature is presented. Besides, Fig. 9 also shows the conventional offline SFRA signature (the excitation is injected through the bushing terminal). It should be noted that the tested transformer is quite different from that of the simulated transformer; thus, the tested FRA signature of Fig. 9 and the simulated FRA signature of Fig. 5 are diverse. It also should be noted that the usage of CCS has a large impact on the online FRA signature, and the low frequency data of the FRA signature is lost, which is the inherent drawback of online FRA method. The gain of the online FRA signature has a rising trend with the increase of frequency in low frequency band. A detailed explanation of the aforementioned points can be found in [19] and [23]. In addition, note that the online IFRA signature is an infrequent signature with few resonant points. The reason is the capacitance formed by CCS of the LV bushing is quite small, and the corner frequency at which the impedance of bushing capacitive coupling circuit is equal to that of transformer winding is as high as 700 kHz. Thus, the trend of the online FRA signature is entirely different from that of the offline signature within 1 ∼ 700 kHz; however, the two signatures are similar beyond 700 kHz.

Turning to the focus of this paper, Fig. 9 indicates that the CCWT-based online IFRA signature is almost overlapped with the online SFRA signature, which confirms that the online IFRA signature can be obtained by the proposed

CCWT from an experimental point of view. Additionally, the CCWT-based online IFRA signature is clearer than the FFT-based online IFRA signature, especially for the anti-resonance at approximately 780 kHz, where redundant oscillations are found in the FFT-based signature. Throughout the entire FFT-based online IFRA signature, there exist massive oscillations. If the operator has no original SFRA data, then these oscillations could be mistaken for the resonant points, which in turn will induce a mistaken diagnosis. Fig. 10 shows the same CCWT-based IFRA signature and the FFT-based signature, but with the upper frequency increased to 3000 kHz. It can be seen that the CCWT-based IFRA signature is still smooth and clear, whereas the FFT-based IFRA signature is completely noisy, and the effective resonant points cannot be directly obtained.

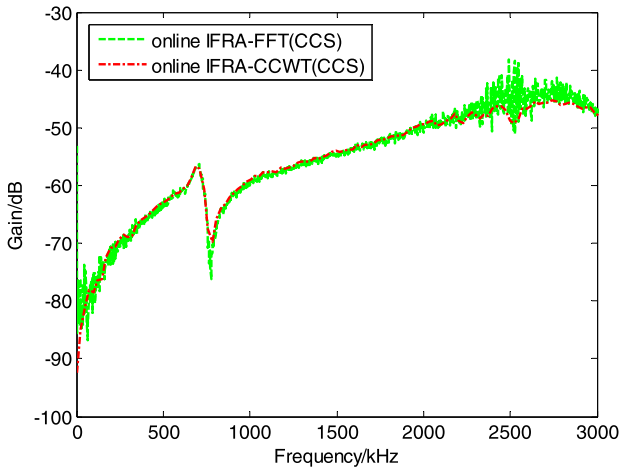

FIGURE 10. Data processing result of online experiment with transformer non-energized (0 ∼ 3000 kHz).

Tab. 3 quantitatively shows the characteristics of the online IFRA signatures, where the resonant frequency of signatures corresponding to three methods are presented. Additionally, to validate the superiority of the CCWT algorithm, taking the online SFRA signature as the reference, the similarities of the online SFRA signature and the online IFRA signatures obtained from FFT and CCWT are compared. Considering that the distribution and length of the frequency points that correspond to the three methods are not totally identical, the statistical indicators, such as the correlation coefficient, cannot be directly calculated to judge the similarity of any two FRA signatures; thus, the area that consists of the region between the signature and the frequency axis is calculated using the trapezoidal integration method. An area variation indicator of the IFRA signature and the SFRA signature is introduced; the result is also shown in Tab. 3. The area variation indicator that corresponds to the CCWT-based signature is 0.6%, whereas the indicator that corresponds to the FFT-based signature is 2.6%. Both the resonant frequencies and the area variation indicator indicate that the CCWT-based online IFRA signature is closer to the online SFRA signature compared with the traditional FFT algorithm. Moreover, the online IFRA signature obtained by CCWT is much clearer and less distorted by the external noise. The proposed CCWT method is more suitable for processing the transient signal to obtain the correct IFRA signature.

TABLE 3. Comparison of experimental results processed by three methods.

Algorithm	f_1(kHz)	f_1'(kHz)	Area variation (%)
Online SFRA	700	782.6	/
Online IFRA-CCWT	695.1	784	0.6
Online IFRA-FFT	705.1	775.1	2.6

B. ONLINE EXPERIMENT WITH TRANSFORMER ENERGIZED

An actual online experiment with transformer energized was also carried out to further verify the proposed CCWT algorithm. The tested transformer was an 11 kV/412 V, three-phase, shell-type transformer, with rated frequency of 50 Hz and connection sets of Dyn1. Specifically, the tested transformer is not identical to the transformer measured in part A of this section. The wiring diagram of the online experiment and the image of field test are shown in Fig. 11 and 12, respectively. In the online experiment, the HV windings were energized by a three-phase symmetric power source with voltage magnitude of 11 kV (RMS of line to line voltage). The LV windings were connected with three-phase resistor loads, each resistance is 2 kΩ. The CCS was mounted on the phase a bushing of the LV windings. The excitation nanosecond pulses with amplitude of 1 kV and pulse width of 200 ns were injected through the CCS. The current of grounded neutral line was measured by a Pearson 7790 current transducer as the response signal. Typical time domain waveforms of the input voltage and the output neutral current are shown in Fig. 13. For comparison, the conventional offline experiment, in which the excitation pulse was injected through the bushing terminal, was also performed on the phase a winding. The offline IFRA signature was calculated by FFT, as presented in Fig. 14. It is noted that the SNR of response signal is high

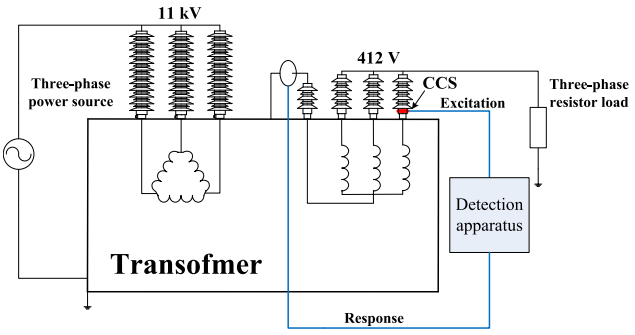

FIGURE 11. Wiring diagram of online experiment with transformer energized.

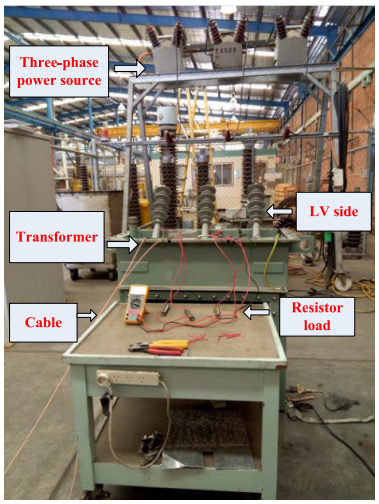

FIGURE 12. Image of field online experiment with transformer energized.

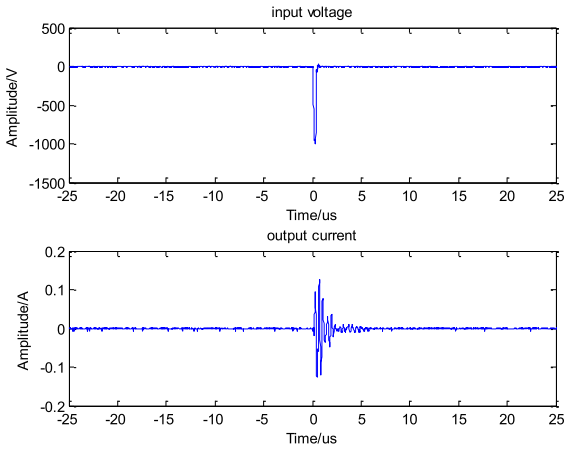

FIGURE 13. Typical time domain waveforms of input voltage and output current of online experiment with transformer energized.

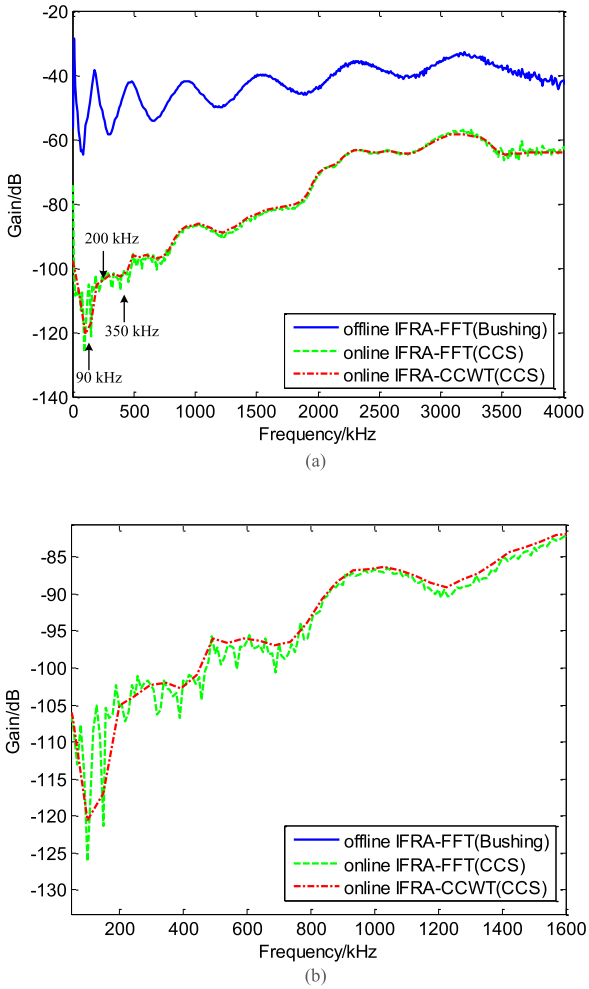

FIGURE 14. Data processing result of online experiment with transformer energized. (a) 0 ∼ 4000 kHz, (b) 20 ∼ 1600 kHz.

enough because of the direct injection of the excitation signal, the offline IFRA signature obtained by FFT is also clear and stable, and can be used as the basis for comparison.

In the online experiment, the measured transient signals were analyzed, multi scale CCWT and FFT algorithms were used to process the experimental data, and two online IFRA signatures were obtained, as shown in Fig. 14. The explanations for the amplitude variance of the offline signature and the online signature can be found in [19]. Fig. 14 shows that the CCWT-based online IFRA signature is much clearer than the FFT-based signature. In particular, for the resonance at approximately 200 kHz and anti-resonances at approximately 90 kHz and 350 kHz, the FFT-based online IFRA signature is completely noisy, and the resonant points cannot be easily distinguished. In contrast, the CCWT-based online IFRA signature is relatively less affected by the noise in the corresponding frequency bands, and the frequencies of resonance and anti-resonance are nearly identical with those of the offline IFRA signature. Again, the data processing result of the online experiment with transformer energized indicates the superiority of the multi scale CCWT algorithm compared to the FFT algorithm regarding the ability to obtain online IFRA signatures from the transient signals.

C. TRANSFORMER EMULATED WINDING DEFORMATION FAULT

In this section, the winding disk space variation fault was emulated in the HV winding of specifically manufactured transformer proposed in section A of this chapter. According to [5], the winding disk space variation fault mainly induces the variation of disk space capacitance, a capacitor is then connected to the connectors of continuous disks to emulate winding disk space variation fault, as shown in Fig. 15. First, the offline SFRA method was performed on the healthy transformer. The transformer was then energized by three phases power frequency power source, and the transient excitation signal and response signal of HV neural point were recorded. These signals were processed by FFT and CCWT, and online IFRA signatures were obtained and shown in Fig. 16. It was also found that the CCWT-based signature is clear and has

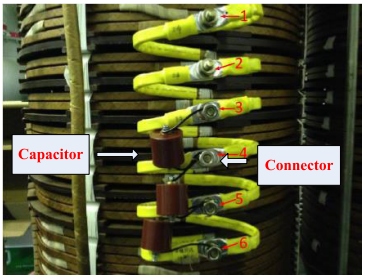

FIGURE 15. Image of emulating winding disk space variation fault.

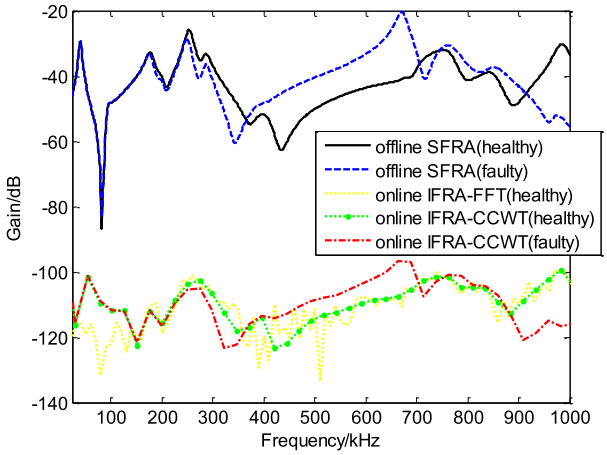

FIGURE 16. Offline SFRA and online IFRA signatures of healthy and faulty transformer.

almost the same trend with the offline SFRA signature regardless of their constant gain difference. While the FFT-based signature has similar trend with offline SFRA signature, but the signature is mask, and there exist some extra resonant points. Second, the middle winding disks were connected with 400 pF capacitors. The offline SFRA signature of emulated fault transformer was obtained. The online experiment was also performed on emulated fault transformer, and the CCWT algorithm was used to obtain the online IFRA signature, as also shown in Fig. 16. It is shown that the online IFRA CCWT-based signature of faulty transformer changes notably in the middle and high frequency bands, the signature shifts toward the low frequency band, compared with the healthy one. This variation is almost identical with the variation of offline SFRA signatures, which indicates that the winding deformation fault can be effectively detected by the online IFRA methd with CCWT algorithm. What's more, compared with FFT-based signature, the online IFRA CCWT-based signature is more clear and accurate.

V. CONCLUSION

An improved signal processing method based on multi scale CCWT was proposed to solve the shortcomings of conventional FFT on obtaining the IFRA signature from the transient signals in online IFRA. The selection of the criteria for the mother wavelet was briefly introduced.

An equivalent electrical model of the transformer winding was simulated, and the cubic spline interpolation was used to pre-process the transient signals to obtain the uniformly spaced sampling data. The noise adding technique was used for obtaining noisy signals with different values of the SNR. The SFRA signature was simulated, and the CCWT and FFT were then used to process the data and obtain the IFRA signatures. The similarity of the CCWT-based signature and the SFRA signature obtained from the noiseless signal indicated the effectiveness of the proposed method, while the smooth characteristic of the CCWT-based IFRA signature obtained from the noisy signal demonstrated the superiority of CCWT than FFT.

In the "online experiment" with the transformer non-energized, the impulse and sweep frequency excitations were injected to a transformer through the CCS, and online SFRA and IFRA signatures were obtained based on three algorithms. Both the resonant frequency and the area variation indicator showed the CCWT-based online IFRA signature is closer to the online SFRA signature. Additionally, CCWT-based signature was found to be much clearer compared with that of FFT-based algorithm.

In the online experiment with the transformer energized, the LV winding was measured with the transformer energized in the HV side. Again, the online IFRA signatures were measured and calculated based on FFT and CCWT algorithms from the transient signals. The analysis result once again showed that the CCWT-based signature is much clearer than the FFT-based signature, and the information of the main resonant points is not distorted, which indicates the superiority of the proposed method.

In transformer emulated winding deformation fault experiment, the offline SFRA and online IFRA signatures of healthy and faulty transformer were obtained and compared. The result indicates that the winding deformation fault can be effectively detected by the online IFRA method with CCWT algorithm. What's more, compared with FFT-based signature, the online IFRA CCWT-based signature is clear and accurate.

REFERENCES

[1] M. Bagheri, M. S. Naderi, T. Blackburn, and T. Phung, "Frequency response analysis and short-circuit impedance measurement in detection of winding deformation within power transformers," *IEEE Elect. Insul. Mag.*, vol. 29, no. 3, pp. 33–40, May 2013.

[2] H.-M. Ahn, Y. H. Oh, J.-K. Kim, J.-S. Song, and S.-C. Hahn, "Experimental verification and finite element analysis of short-circuit electromagnetic force for dry-type transformer," *IEEE Trans. Magn.*, vol. 48, no. 2, pp. 819–822, Feb. 2012.

[3] M. Wang, "Winding movement and condition monitoring of power transformers in service," Ph.D. dissertation, Dept. Elect. Comput. Eng., Univ. British Columbia, Vancouver, BC, Canada, 2003.

[4] M. Bagheri, A. Zollanvari, and S. Nezhivenko, "Transformer fault condition prognosis using vibration signals over cloud environment," *IEEE Access*, vol. 6, pp. 9862–9874, 2018.

[5] A. Abu-Siada, N. Hashemnia, S. Islam, and M. A. S. Masoum, "Understanding power transformer frequency response analysis signatures," *IEEE Elect. Insul. Mag.*, vol. 29, no. 3, pp. 48–56, May 2013.

[6] H. Rahbarimagham, H. K. Porzani, M. S. A. Hejazi, M. S. Naderi, and G. B. Gharehpetian, "Determination of transformer winding radial deformation using UWB system and hyperboloid method," *IEEE Sensors J.*, vol. 15, no. 8, pp. 4194–4202, Aug. 2015.

[7] E. Arri, A. Carta, F. Mocci, and M. Tosi, "Diagnosis of the state of power transformer windings by on-line measurement of stray reactance," *IEEE Trans. Instrum. Meas.*, vol. 42, no. 2, pp. 372–378, Apr. 1993.
[8] B. García, J. C. Burgos, and Á. Alonso, "Winding deformations detection in power transformers by tank vibrations monitoring," *Electr. Power Syst. Res.*, vol. 74, no. 1, pp. 129–138, 2005.
[9] S. Mortazavian, M. M. Shabestary, Y. A.-R. I. Mohamed, and G. B. Gharehpetian, "Experimental studies on monitoring and metering of radial deformations on transformer HV winding using image processing and UWB transceivers," *IEEE Trans. Ind. Informat.*, vol. 11, no. 6, pp. 1334–1345, Dec. 2015.
[10] A. Abu-Siada and S. Islam, "A novel online technique to detect power transformer winding faults," *IEEE Trans. Power Del.*, vol. 27, no. 2, pp. 849–857, Apr. 2012.
[11] V. Behjat, A. Vahedi, A. Setayeshmehr, H. Borsi, and E. Gockenbach, "Diagnosing shorted turns on the windings of power transformers based upon online FRA using capacitive and inductive couplings," *IEEE Trans. Power Del.*, vol. 26, no. 4, pp. 2123–2133, Oct. 2011.
[12] R. K. Senobari, J. Sadeha, and H. Borsi, "Frequency response analysis (FRA) of transformers as a tool for fault detection and location: A review," *Electr. Power Syst. Res.*, vol. 155, pp. 172–183, Feb. 2018.
[13] M. Bagheri, S. Nezhivenko, B. T. Phung, and T. Blackburn, "Air core transformer winding disk deformation: A precise study on mutual inductance variation and its influence on frequency response spectrum," *IEEE Access*, vol. 6, pp. 7476–7488, 2018.
[14] E. Gomez-Luna, G. A. Mayor, C. Gonzalez-Garcia, and J. P. Guerra, "Current status and future trends in frequency-response analysis with a transformer in service," *IEEE Trans. Power Del.*, vol. 28, no. 2, pp. 1024–1031, Apr. 2013.
[15] T. Leibfried and K. Feser, "Monitoring of power transformers using the transfer function method," *IEEE Trans. Power Del.*, vol. 14, no. 4, pp. 1333–1341, Oct. 1999.
[16] M. Wang, A. J. Vandermaar, and K. D. Srivastava, "Condition monitoring of transformers in service by the low voltage impulse test method," in *Proc. Int. Symp. High Voltage Eng. (ISH)*, London, U.K., 1999, pp. 45–48.
[17] T. D. Rybel, A. Singh, J. A. Vandermaar, M. Wang, J. R. Marti, and K. D. Srivastava, "Apparatus for online power transformer winding monitoring using bushing tap injection," *IEEE Trans. Power Del.*, vol. 24, no. 3, pp. 996–1003, Jul. 2009.
[18] C. Yao *et al.*, "Transformer winding deformation diagnostic system using online high frequency signal injection by capacitive coupling," *IEEE Trans. Dielectr. Electr. Insul.*, vol. 21, no. 4, pp. 1486–1492, Aug. 2014.
[19] M. Bagheri, M. S. Naderi, T. Blackburn, and B. T. Phung, "Bushing characteristic impacts on on-line frequency response analysis of transformer winding," in *Proc. IEEE Int. Conf. Power Energy (PECon)*, Kota Kinabalu, Malaysia, 2012, pp. 956–961.
[20] B. Mohseni, N. Hashemnia, and S. Islam, "Application of S transform for detection of external interferences in online transformer impulse frequency response analysis," in *Proc. IEEE Int. Conf. Environ. Elect. Eng., IEEE Ind. Commercial Power Syst. Eur. (EEEIC/I&CPS Europe)*, Milan, Italy, Jun. 2017, pp. 1–4.
[21] E. Gómez-Luna, G. A. Mayor, J. P. Guerra, D. F. S. Salcedo, and D. H. Gutiérrez, "Application of wavelet transform to obtain the frequency response of a transformer from transient signals—Part 1: Theoretical analysis," *IEEE Trans. Power Del.*, vol. 28, no. 3, pp. 1709–1714, Jul. 2013.
[22] E. G. Luna, G. A. Mayor, and J. P. Guerra, "Application of wavelet transform to obtain the frequency response of a transformer from transient signals—Part II: Practical assessment and validation," *IEEE Trans. Power Del.*, vol. 29, no. 5, pp. 2231–2238, Oct. 2014.
[23] M. Bagheri, S. Nezhivenko, and B. T. Phung, "Loss of low-frequency data in on-line frequency response analysis of transformers," *IEEE Elect. Insul. Mag.*, vol. 33, no. 5, pp. 32–39, Sep./Oct. 2017.
[24] C. Li *et al.*, "Impact analysis of the capacitive coupling sensor on bushing external insulation," *IET Gener., Transmiss. Distrib.*, vol. 10, no. 14, pp. 3663–3670, 2016.
[25] A. Setayeshmehr, H. Borsi, E. Gockenbach, and I. Fofana, "On-line monitoring of transformer via transfer function," in *Proc. IEEE Elect. Insul. Conf. (EIC)*, May/Jun. 2009, pp. 278–282.
[26] E. Rahimpour, J. Christian, K. Feser, and H. Mohseni, "Transfer function method to diagnose axial displacement and radial deformation of transformer windings," *IEEE Trans. Power Del.*, vol. 18, no. 2, pp. 493–505, Apr. 2003.
[27] S. Bagheri, Z. Moravej, and G. B. Gharehpetian, "Classification and discrimination among winding mechanical defects, internal and external electrical faults, and inrush current of transformer," *IEEE Trans. Ind. Informat.*, vol. 14, no. 2, pp. 484–493, Feb. 2018.
[28] C. Duarte, P. Delmar, K. W. Goossen, K. Barner, and E. Gomez-Luna, "Non-intrusive load monitoring based on switching voltage transients and wavelet transforms," in *Proc. Int. Workshop Future Instrum.*, Oct. 2012, pp. 1–4.
[29] N. Hashemnia, A. Abu-Siada, and S. Islam, "Improved power transformer winding fault detection using FRA diagnostics—Part 1: Axial displacement simulation," *IEEE Trans. Dielectr. Electr. Insul.*, vol. 22, no. 1, pp. 556–563, Feb. 2015.
[30] O. Aljohani and A. Abu-Siada, "Application of digital image processing to detect short-circuit turns in power transformers using frequency response analysis," *IEEE Trans. Ind. Informat.*, vol. 12, no. 6, pp. 2062–2073, Dec. 2016.

ZHONGYONG ZHAO was born in Guangyuan, Sichuan, China. He received the B.Sc. and Ph.D. degrees in electrical engineering from Chongqing University, Chongqing, China, in 2011 and 2017, respectively. He received the scholarship from the China Scholarship Council to enable him to attend a joint-training Ph.D. program at Curtin University, Perth, Western Australia, in 2015-2016. He is currently an Associate Professor with the College of Engineering and Technology, Southwest University, Chongqing. His areas of research include condition monitoring and fault diagnosing for HV apparatus, and pulsed power technology.

CHAO TANG was born in Sichuan, China, in 1981. He received the M.S. and Ph.D. degrees in electrical engineering from Chongqing University, China, in 2007 and 2010, respectively. As a Ph.D. student from 2008 to 2009, and as a Visiting Scholar from 2013 to 2013 and from 2015 to 2016, he studied in The Tony Davies High Voltage Laboratory, University of Southampton, U.K., doing some researches on the dielectric response characteristics and space charge behaviors of oil-paper insulation. He is currently an Associate Professor with the College of Engineering Technology, Southwest University, China. His research activities are mainly in the field of online monitoring of insulation conditions and fault diagnosis for high-voltage equipment.

CHENGUO YAO (M'08) was born in Nanchong, Sichuan, China. He received the B.S., M.S., and Ph.D. degrees in electrical engineering from Chongqing University, Chongqing, China, in 1997, 2000, and 2003, respectively. He became a Professor with the School of Electrical Engineering, Chongqing University, in 2007. He has been a Visiting Scholar with Old Dominion University, Norfolk, VA, USA, from 2017 to 2018. His current works include online monitoring of insulation condition and insulation fault diagnosis for HV apparatus, pulsed power technology and its application in biomedical engineering.

QU ZHOU was born in Sichuan Province, China, in 1983. He received the B.Sc. degree in biomedical engineering and the Ph.D. degree in electrical engineering from Chongqing University, China, in 2007 and 2014, respectively. He is currently an Associate Professor with the College of Engineering and Technology, Southwest University, and also a Visiting Scholar with Wayne State University, Detroit, MI, USA. He has authored over 30 papers based on his professional work. His main research interests include high-voltage technology, insulation online monitoring, fault diagnosis, and condition-based maintenance of power equipment.

LINGNA XU received the B.Sc. degree from the University of Science and Technology, Beijing, in 2008, the M.Sc. degree from the Polytechnic Institute of New York University, in 2010, and the Ph.D. degree in electrical engineering from Chongqing University. She is currently a Lecturer with the Department of Electrical Engineering, College of Engineering and Technology, Southwest University. Her main research interests include online monitoring and fault diagnosis of power equipment, condition-based maintenance, and the internal insulation and thermal properties of power transformers.

YINGANG GUI was born in Chongqing, China, in 1988. He received the B.Sc. degree in applied physics from Chongqing Normal University in 2011 and the Ph.D. degree in electrical engineering from Chongqing University in 2017. He was a recipient of the Chinese Government Scholarship to sponsor the joint training program as a Ph.D. in the Georgia Institute of Technology, Atlanta, GA, USA. He studies high-voltage electric equipment insulation online monitoring and fault diagnosis.

SYED ISLAM (M'83–SM'93) received the B.Sc. degree in electrical engineering from the Bangladesh University of Engineering and Technology, Bangladesh, in 1979, the M.Sc. and Ph.D. degrees in electrical power engineering from the King Fahd University of Petroleum and Minerals, Dhahran, Saudi Arabia, in 1983, and 1988, respectively.

He was a keynote speaker and an invited speaker at many international workshops and conferences. He is currently the John Curtin Distinguished Professor of electrical power engineering and the Director of the Centre for Smart Grid and Sustainable Power Systems, Curtin University, Perth, Australia. He has been a Visiting Professor with the Shanghai University of Electrical Power, China. He has authored over 300 technical papers in his area of expertise. His research interests are in condition monitoring of transformers, wind energy conversion, and smart power systems. He was a recipient of the Dean's Medallion for research at Curtin University in 1999, the IEEE T Burke Haye's Faculty Recognition Award in 2000, the Curtin University Inaugural Award for Research Development in 2012, and the Sir John Madsen Medal in 2011 and 2014 for the best electrical engineering paper in Australia.

He is also the Dean International for the Faculty of Science and Engineering, Curtin University. He is a member of the steering Committee of the Australian Power Institute and a member of the WA EESA Board. He is a Fellow of the Engineers Australia, a Senior Member of the IEEE IAS, PES, and DEIS, a Fellow of the IET and a Chartered Engineer in the United Kingdom. He is a founding Editor of the *IEEE Transactions on Sustainable Energy* and an Associate Editor of the *IET Renewable Power Generation*. He was the Guest Editor-in-Chief for the *IEEE Transactions on Sustainable Energy* special issue on Variable Power Generation Integration into Grid.